Interval Approach to Identification of Catalytic Process Parameters*

Sergey I. Kumkov†

Institute of Mathematics and Mechanics,
Ural Branch of Russian Academy of Sciences, and
Ural Federal University, Institute of
Radio-Electronics and Informational Technologies,
Ekaterinburg, Russia
kumkov@imm.uran.ru

Yuliya V. Mikushina‡

Institute of Organic Synthesis,
Ural Branch of Russian Academy of Sciences,
Ekaterinburg, Russia
mikushina2006@mail.ru

Abstract

The paper deals with applications of interval analysis methods to a special practical problem of parameter identification of a real chemical catalytic process. Several possible models of the process are given. The measured data of the process are corrupted by both usual fluctuation errors and chaotic disturbances. Samples of the input information are short. Any characteristics (including probabilistic ones) of corruptions are unknown, but the total corruption in each measurement is assumed to be bounded. As the result, the identification of model parameters under the uncertainty is performed by interval methods. The output results are represented in the form of the information sets (membership sets) of admissible values of the parameters.

Keywords: interval identification, parameters, model, experimental process
AMS subject classifications: 65G40, 93A30

*Submitted: November 9, 2012; Revised: September 22, 2013; Accepted: November 7, 2013.

†S. I. Kumkov was supported by the RFBR grants Nos. 12-01-00537 and 13-01-96055.

‡Yu. V. Mikushina was supported by the UrB RAS grant No. 12-I-3-2058 (State Registr. No. 01201252834).

1 Introduction

The overwhelming majority of methods used in practice for processing corrupted experimental data are based on the mathematical statistics and regression approaches (see, e.g., Russian Standards [1]–[3]). For their application, these approaches need the following crucial assumptions on properties of corruption in the data to be processed:

1) the measurement sample is representative and has sufficient length;
2) the total error (in measurement) has a probabilistic character;
3) as a rule, probability distributions of the total error are assumed to be Gaussian;
4) there are no chaotic components (shifts) in measurements;
5) errors in sequential measurements are independent.

The results from these approaches are represented as point-wise estimations of the vectors of parameters with their confidential intervals.

Unfortunately in practice, we often encounter an absolutely different situation:

1) the sample is too short and comprises only a few measurements;
2) there is no information about the properties of all components of the total error, especially about the probabilistic ones, and errors are hardly Gaussian;
3) experimental measurements contain not only usual fluctuating components, but also apparently chaotic ones (or suspicious shifts) with unknown properties;
4) nothing can be said about dependence of errors in sequential measurements.

Nevertheless, researchers formally apply the regression approach, although the parameter estimates can have only a qualitative character, and it is impossible to introduce any (valid) confidence interval probabilities or to give any confidence intervals. We also note that, assuming a Gaussian distribution of errors, classical statistical and regression approaches cannot take into account the important fact of the physical boundedness of the total corruption in measurements.

An introduction of idea of physically bounded corruption without any probabilistic properties leads directly to application of interval analytic approaches. In practice, a researcher may know approximately the value of this bound and can choose a reasonable value. Hence, this value is assumed to be a free variable similar to the confidence interval probability in the statistical approaches. Furthermore, the output results are represented in the form of the information (membership) sets of admissible values of parameters.

The paper has the following structure. Section 2 describes the chemical experiment, input information, and possible models (of research interest) of the process. We describe results of previous analyses of the validity of the standard approach for given models. In Section 3, interval analysis application features are considered, and the problem formulation is given. Section 4 presents the interval analysis techniques used for identification. Section 5 describes results of processing the experimental data by the elaborated interval approaches.

2 Experiment, Input Data, and Models

The results of measuring the chemical process of catalytic decomposition [4] for three catalysts are considered (see Fig. 1): 1) $K_xLi_yWO_3$ (nano-sized); 2) Na_xWO_3; 3) $K_{0.475}WO_3$. Measurements are marked by circles, squares, and triangles, respectively.

Properties of these catalysts (including the most advanced ones, called active nano-sized catalysts) are well investigated. Usually, we know the graph of the process,

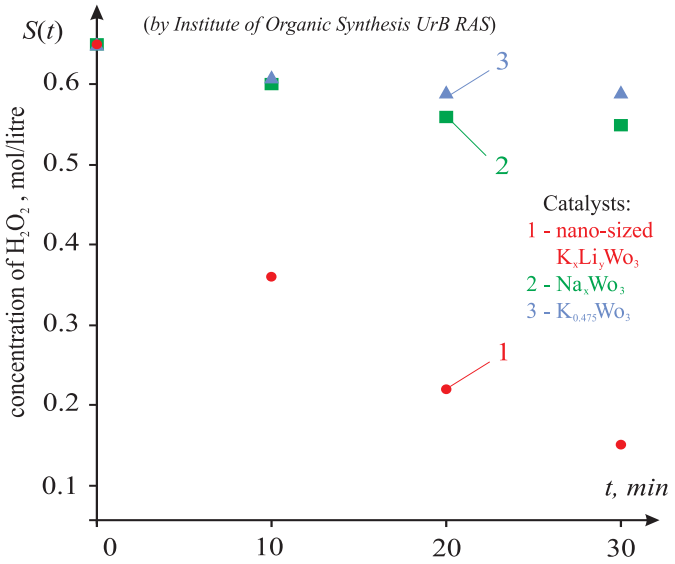

Figure 1: Experimental data; decomposition of H_2O_2 on bronzes (kinetic curves).

the values of its parameters, and activity (the process of the derivative). For each experiment, a sample of measurements contaminated with noise is given. Conditions of the experiments are: fixed volume and initial concentration of the standard reactant H_2O_2, fixed volume and initial concentration of various catalysts to be tested, the same (standard) environmental conditions of the experiment (temperature, pressure, etc.), and the same (standard) procedures of measuring the reactant concentration versus the time of the decomposition reaction.

On the whole, the experiments have been performed very carefully with very clear reactants and small actual measurement errors. As a consequence (Fig. 1), the measurements go without jerks, *i.e.,* there are no evident outliers in the samples.

Input data and model of corruption. The values t_n of the independent argument (time) are assumed to be known exactly, but an observation of the reaction is performed on relatively short time interval. The sample is very short; there are only four measurements. The measurement of the process is indirect, implying the presence not only of the usual fluctuation errors, but also of additional possible chaotic corruptions in the measured values of the reactant concentration. It is assumed that measurements in the sample are contaminated with total additive noise bounded by modulus; no probabilistic information is known. The model of corruption has the form:

$$\begin{aligned} &s_n = s_n^* + e_n, \qquad n = \overline{1,N}, \qquad N = 4, \\ &e_n = e_n^* + \chi_n, \qquad |e_n| \le e_{\max}, \end{aligned} \tag{1}$$

where s_n is a corrupted measurement, s_n^* is the unknown true value being measured, e_n is the *absolute* total error (corruption) independent of the measured value and bounded in modulus by the value $e_{\max}$, *i.e.,* an approximate *a priori* total accuracy of measurement assumed to be known, e_n^* is the usual fluctuating measurement component of the total error, χ_n is a chaotic component. *No assumptions* on probabilistic

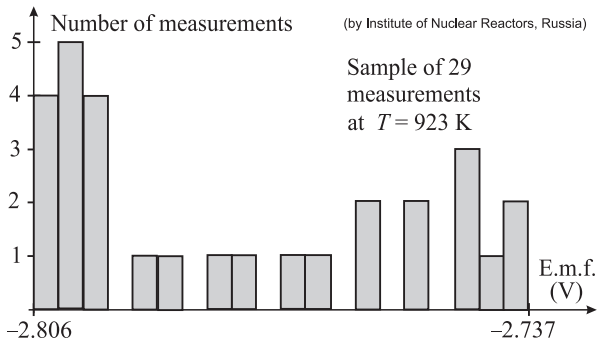

Figure 2: Experimental histogram of non-Gaussian and unstable form.

characteristics of the total error are made. In practice, such a refusal can be substantiated by the fact that the experimental histograms of measurement dissipation do not have the Gaussian character (see Fig. 2, in which some constant EMF is measured) and often are not stable from one experiment to another.

Several hierarchical models of the process have been investigated [4]–[7].

Model 1. An experimental process is described by a third order polynomial

$$S(t, a_0, a_1, a_2, a_3) = a_0 + a_1 t + a_2 t^2 + a_3 t^3. \tag{2}$$

Here, the vector of parameters to be identified is four-dimensional: $\{a_0, a_1, a_2, a_3\}$. Usually, this model is aimed only at analysis of the process trend.

Model 2. An experimental process is described by a single exponent

$$S(t, A, \alpha) = A \exp(\alpha t). \tag{3}$$

Here, the vector of parameters to be identified is two-dimensional: $A > 0$ is the initial value of concentration, and $\alpha < 0$ is the coefficient of activity in an approximate model. This model is also aimed at analysis of the process trend.

Model 3. An experimental process is described by the function

$$S(t, A, \alpha, B) = A \exp(\alpha t) + B. \tag{4}$$

Here, the vector of parameters to be identified is three-dimensional: $A > 0$ is the initial value of concentration, $\alpha < 0$ is the activity coefficient, and $B > 0$ is the background value. This model is chosen for more detailed analysis of the process.

Model 4. The function that describes an experimental process has the form

$$S(t, A, \alpha, \beta, B) = A \exp(\alpha t + \beta t^2) + B. \tag{5}$$

Here, the vector of parameters to be identified is four-dimensional: $A > 0$ is the initial value of concentration, $\alpha < 0$ is the coefficient of activity of the first order, $\beta < 0$ is the coefficient of activity of the second order, and $B > 0$ is the background value. This model is used for detailed analysis of the process, especially in estimation of the nano-sized catalyst activity.

Previous analysis of validity of the standard least squares mean (LSQ-method) and various models was performed (Figs. 3–6). For Model 1, the LSQ-method produces (Fig. 3) invalid results that do not conform in the physical sense. When applied to Model 2 (Fig. 4), it shows its invalidity and the invalidity of this model since its poor approximation contradicts the high accuracy of the process implementation, *i.e.,* gives unacceptable (in the experience of the researchers) and incomplete estimations. For Model 3 (Fig. 5), the results seem to be satisfactory, but incomplete. For Model 4 (Fig. 6), the results are unacceptable, because the LSQ-method is not valid. Note that incompleteness of results is stipulated by an absence of the probability characteristics of the total error in the input data.

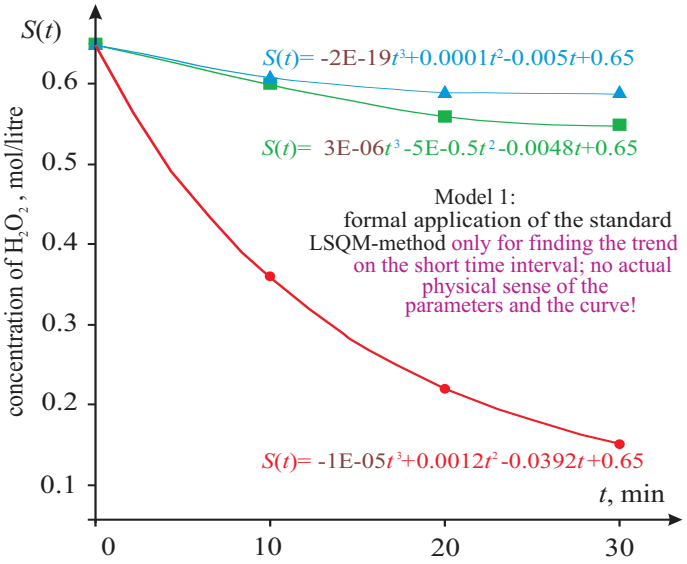

Figure 3: LSQ–approximation; invalidity of the method and Model 1.

3 Interval Analysis Application Features and Problem Formulation

Let us introduce necessary notions of the interval approach to data analysis (see [8]–[10]). We are given:

1) a measurement sample $\{t_n, s_n\}$, $n = \overline{1, N}$;

2) a model of measurement corruption (1) with the interval bound $|e_n| \le e_{\max}$ on the total error;

3) a model of the process, *i.e.,* the *describing function* (*dependence*) $S(t, p)$ with the argument t and the parameter vector p.

We need the following definitions, attempting to follow standard notations [16].

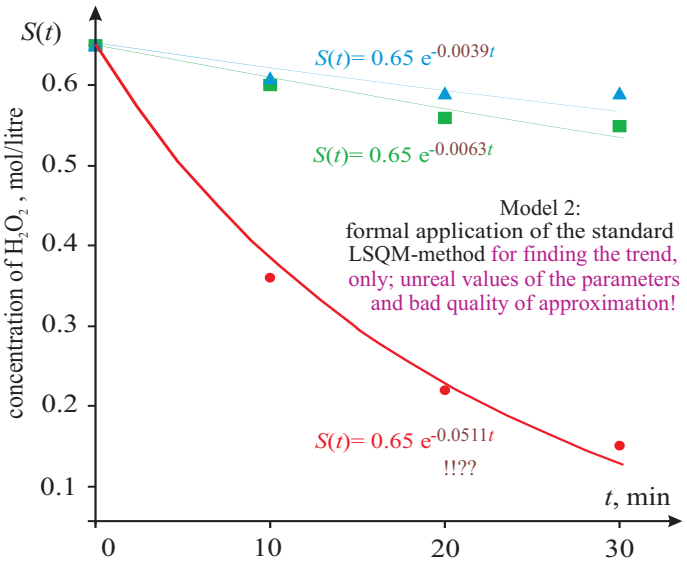

Figure 4: Model 2; LSQ–approximation; unacceptable results.

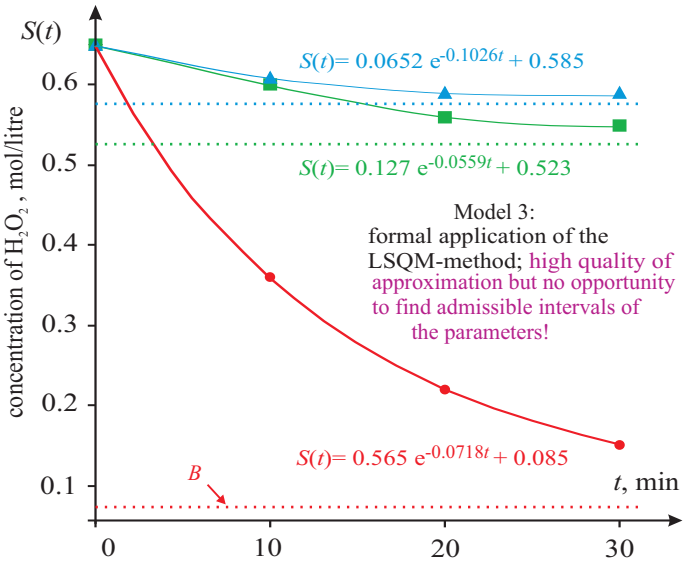

Figure 5: Model 3; LSQ–approximation; incomplete results.

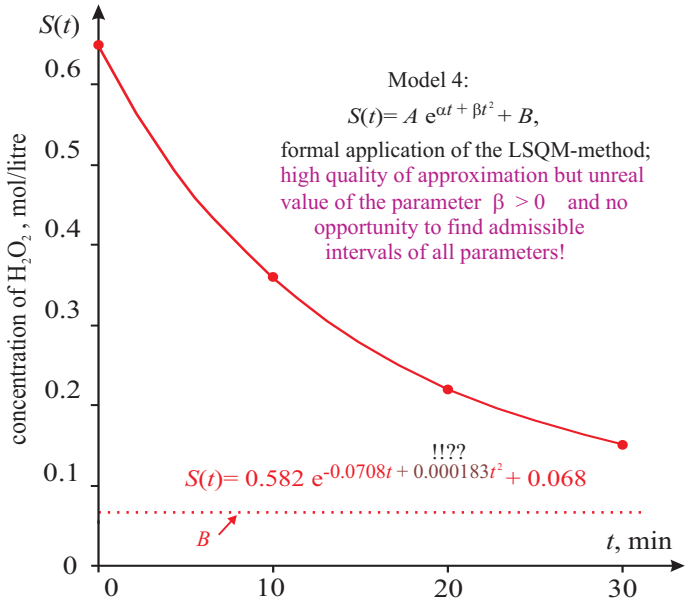

Figure 6: Model 4; LSQ–approximation; unacceptable results.

The *Uncertainty set* of each measurement (USM), *i.e.,* in the case under consideration, the uncertainty interval

$$\boldsymbol{s}_n = [\underline{\boldsymbol{s}}_n, \overline{\boldsymbol{s}}_n] : \quad \underline{\boldsymbol{s}}_n = s_n - e_{\max},\ \overline{\boldsymbol{s}}_n = s_n + e_{\max}, \quad n = \overline{1, N}. \tag{6}$$

The *Admissible value* p of the parameter vector and corresponding *admissible dependence*

$$\big(p, S(t,p)\big) : \ S(t_n, p) \in \boldsymbol{s}_n, \quad \text{for all } n = \overline{1, N}. \tag{7}$$

The *Information set* (INFS, the membership set), *i.e.*, the totality of all values p, for which

$$\boldsymbol{I}(e_{\max}, p) = \big\{p : S(t_n, p) \in \boldsymbol{s}_n, \quad \text{for all } \ n = \overline{1, N}\big\}. \tag{8}$$

The *Consistent* (*inconsistent*) sample

$$\begin{array}{c} \text{if for the given } e_{\max} : \ \boldsymbol{I}(e_{\max}, p) \neq \varnothing, \\ (\text{if for the given } e_{\max} : \ \boldsymbol{I}(e_{\max}, p) = \varnothing. \end{array} \tag{9}$$

The *tube of admissible dependences*, *i.e.,* the totality of all the dependences (functions) for which

$$\boldsymbol{T}(t) = \big\{S(t,p) : S(t_n, p) \in \boldsymbol{s}_n, \quad \text{for all } \ n = \overline{1, N}, \ \text{and } p \in \boldsymbol{I}(e_{\max}, p)\big\}. \tag{10}$$

Figure 7a and 7b illustrations the introduced concepts above.

Formulation of the problem: *Identify and* (*construct*) *the set of admissible values of the model parameters consistent with the given input data under uncertainty.*

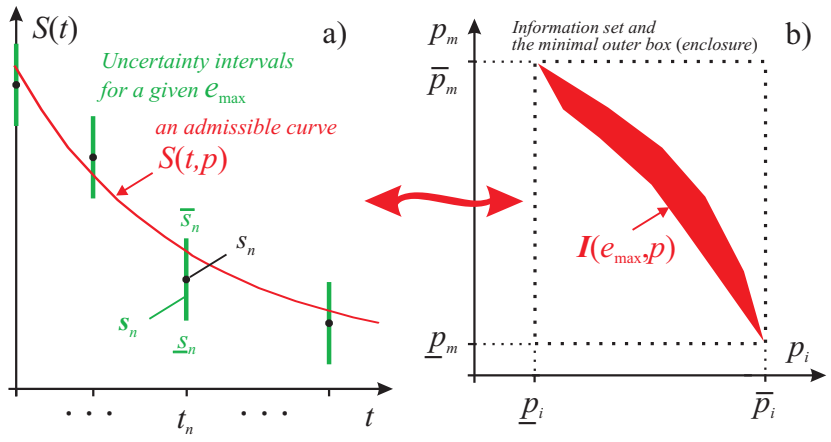

Figure 7: Illustrations to the main notions.

4 Interval Analysis Techniques

After rejecting the probability-based statistical paradigm and arriving at the interval description of the total corruption in measurements, the situation changes crucially and becomes constructive. As we remarked earlier, the notion of "confidence interval probability" loses its meaning. Its role is played by the bound $e_{\max}$ of a variable level. In contrast to ephemeral "confidence interval probability", the work with the variable value $e_{\max}$ is absolutely understood (in an engineering sense) by researchers.

For general description functions (dependences), there are "classical" interval algorithms based on application of interval boxes [8]–[10] for the approximate building of information sets with any prescribed accuracy. However, constructive application of properties a specific function allows one to formulate algorithms that provide *exact analytical descriptions* of the INFS boundaries and are faster. This is the case when the describing function originally (or after some transformation) *depends linearly* on parameters to be identified (estimated). Typical origins of such transformations are given in [3], and this idea is used in this paper.

Consider the main applications of the interval algorithms described in [12]–[15] on the Model 3. The following procedures are performed.

First, the dependence (4) is transformed from the original form $S(t, A, \alpha, B) = A\exp(\alpha t) + B$ to a linear dependence on parameters $\log A$ and α. Shifting the parameter B to the left-hand side and then taking the natural logarithm of both sides, we obtain the inclusions

$$\boldsymbol{y}(t_n, B, \log A, \alpha) = \log(\boldsymbol{s}_n - B) \ni \log A + \alpha t_n \tag{11}$$

with linear dependence between the parameter α and the new parameter $\log A$. The left-hand side of this membership is an interval for each t_n.

Next, we introduce some reasonable *a priori* interval on the parameter B and supply it with a grid $\{B_m, m = \overline{1, M}\}$:

$$\begin{aligned} &\boldsymbol{B} = [\underline{\boldsymbol{B}}, \overline{\boldsymbol{B}}]: \ \Delta B = (\overline{\boldsymbol{B}} - \underline{\boldsymbol{B}})/(M-1), \\ &B_m = \underline{\boldsymbol{B}} + \Delta B(m-1), \quad m = \overline{1, M}. \end{aligned} \tag{12}$$

Under the circumstances, for each fixed node B_m, we obtain a collection of the interval inclusions for the parameters α and $\log A$ and every t_n:

$$\log A + \alpha t_n \in \log\bigl(\boldsymbol{s}_n - B_m\bigr), \qquad n = \overline{1,N}. \tag{13}$$

Let us illustrate the elaborated interval procedures for parameter estimation on an example of a linear function with a two-dimensional vector (a,b) of parameters. The function is assumed to be given over a grid $\{x_n\}$, $n = \overline{1,N}$, so that

$$y(x_n,a,b) = a + bx_n, \qquad n = \overline{1,N}. \tag{14}$$

Next, we construct the collection of "pairwise" $\{\boldsymbol{G}_{i,n}\}$ *partial information sets* (PINS). Due to properties of the linear dependence (11), we consider a pair $(\boldsymbol{y}_i, \boldsymbol{y}_n)$ of USM's with their endpoints (Fig. 8a, vertical black segments with black circles). Every such pair defines a collection of dependences admissible (*i.e.,* consistent) with these two USMs. The marginal (solid) and intermediate (dots and dashes) lines determine the corresponding quaternary of coefficient points (a_1,b_1)–(a_4,b_4) (Fig. 8a). In the plane of parameters, these points are vertices of the partial information set (Fig. 8b, parallelogram in gray) of the corresponding admissible values of the line parameters. The boundaries of this parallelogram are linear, and they can be described exactly:

$$\boldsymbol{G}_{i,n} = \{a,b : a + bx_i \in \boldsymbol{y}_i \text{ and } a + bx_n \in \boldsymbol{y}_n\}, \qquad i,n = \overline{1,N}, \quad \text{and } n > i. \tag{15}$$

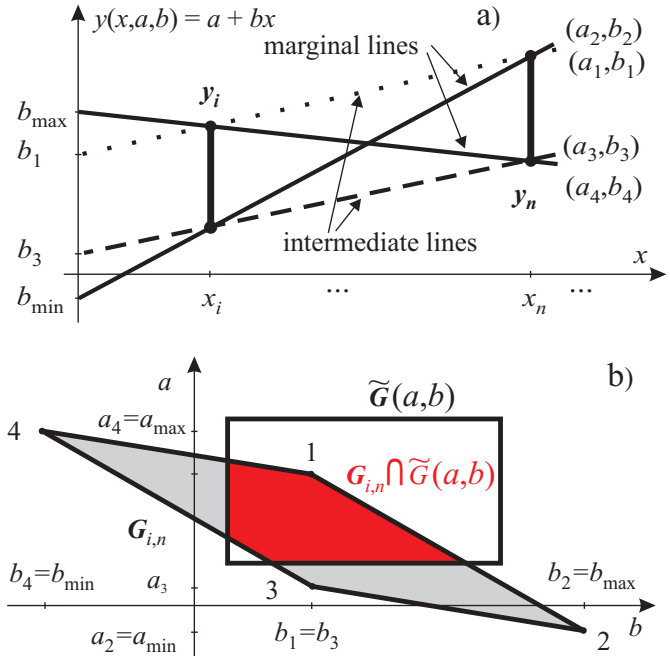

Figure 8: A pair of USMs and its PINS of parameters.

This technique is rather flexible and allows one to take into account any *a priori* information on feasible values of the parameters. Let an *a priori* rectangle $\widetilde{\boldsymbol{G}}(a,b)$ be

given (Fig. 8b). Then, it is possible to enhance the result of estimation (in red) by intersecting the PINS $\boldsymbol{G}_{i,n}$ with $\widetilde{\boldsymbol{G}}(a,b)$. Such a technique can be termed a *partial pairwise adjustment method*. It is similar to techniques from constraint propagation.

Constructing the information set $\boldsymbol{I}(a,b)$ of the parameters a and b for a *consistent* sample is performed by intersecting all PINS's by a standard intersection operation for convex sets:

$$\boldsymbol{I}(a,b) = \bigcap_{i,n=1,\dots,N,\ n>i} \boldsymbol{G}_{i,n}(a,b) = \bigcap_{i\equiv 1,\ n=2,\dots,N} \boldsymbol{G}_{1,n}. \tag{16}$$

The latter equality in this formula is valid for a *linear dependence* on the parameters a and b. Moreover, in this case, the information set is a convex polygon with exact description of linear boundaries between its vertices.

The marginal sections of INFS (16) are calculated using necessary adjustment of the grid $\{B_m\}$: we shift the position of the interval $\boldsymbol{B} = [\underline{\boldsymbol{B}}, \overline{\boldsymbol{B}}]$, change the number of nodes M, and decrease the step ΔB around these sections.

Constructing the tube $\boldsymbol{T}(x)$ of admissible dependences amounts to calculation of the collection of its lower $\underline{T}(x)$ and upper $\overline{T}(x)$ boundary points for each value of the argument x_n, $n = \overline{1,N}$,

$$\underline{T}(x_n) = \min_{(a,b)\in\boldsymbol{I}(a,b)} \{a + bx_n\}, \quad \overline{T}(x_n) = \max_{(a,b)\in\boldsymbol{I}(a,b)} \{a + bx_n\}. \tag{17}$$

For the linear function, the upper (lower) boundaries of the tube over the intervals $[x_n, x_{n+1}]$ are lines that connect the corresponding upper (lower) edges of the cross–sections $[\underline{T}(x_n),\ \overline{T}(x_n)]$ and $[\underline{T}(x_{n+1}),\ \overline{T}(x_{n+1})]$. As a result, the data provided to a user consist of the tube (17), the information set (16), its minimal enclosure box, *i.e.,* intervals $\boldsymbol{a} = [\underline{a}, \overline{a}]$ and $\boldsymbol{b} = [\underline{b}, \overline{b}]$, and the central point $(a_{\mathbf{c}}, b_{\mathbf{c}})$:

$$\begin{aligned}
&\underline{a} = \min\big\{a:\ (a,b)\in\boldsymbol{I}(a,b)\big\},\quad \overline{a} = \max\big\{a:\ (a,b)\in\boldsymbol{I}(a,b)\big\},\\
&\underline{b} = \min\big\{b:\ (a,b)\in\boldsymbol{I}(a,b)\big\},\quad \overline{b} = \max\big\{b:\ (a,b)\in\boldsymbol{I}(a,b)\big\},\\
&a_{\mathbf{c}} = (\underline{a} + \overline{a})/2,\quad b_{\mathbf{c}} = (\underline{b} + \overline{b})/2.
\end{aligned}$$

It can happen that the information set (16) of the whole sample does not exist for a corrupted sample, *i.e.,* the set (16) is empty. This means that for the value of the constraint $e_{\max}$ provided by the researcher, the sample is inconsistent. We have elaborated special algorithms and software [13] based on graph theory that divide such a sample, *inconsistent on the whole*, into a collection of *consistent subsamples* of various lengths. Usually, researchers are interested in a subsample of the maximal length. We do not consider subsamples of unacceptably short length that can be generated by possible outliers.

Remark. *Under the above mentioned uncertainty, there is not enough information to detect reliably detached outliers in the process measurements. Instead, it is suggested to perform analysis of the information sets of subsamples in the space of parameters; this seems to be a constructive approach to remove the influence of possible outliers.*

Recall that the value of the bound $e_{\max}$ is assumed to be known approximately in practice. This parameter is assumed to be free, and we can be vary it. That provides an interesting and useful property of the interval approach we have constructed. Namely, it becomes possible to estimate, from below, the *actual level* of corruption in the given input sample. Let, for the given initial constraint $e_{\max}^{\mathbf{init}}$ on the value of the total

corruption, the input sample (16) be *inconsistent* in spite of absence of "evident" outliers. Then, increasing the constraint from the initial value $e^{\mathbf{init}}_{\max}$, we inevitably arrive at the situation when, for some *critical* value $e^*_{\max}$, the information set becomes *non-empty* and consists of the only point $\boldsymbol{I}(a,b) = (a^*, b^*)$. Such a value $e^*_{\max}$ can be a lower estimate of the actual corruption level in measurements of the input sample.

In the case of an initially consistent sample, the outer estimate (from below) $e^*_{\max}$ of the actual level of corruptions is found similarly by *decreasing* the constraint from its initial value $e^{\mathbf{init}}_{\max}$, as illustrated in Fig. 9.

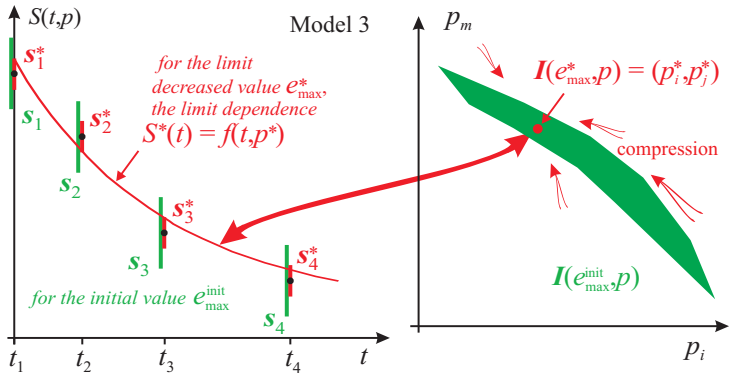

Figure 9: Estimation of the actual level $e^*_{\max}$ of corruptions in the sample.

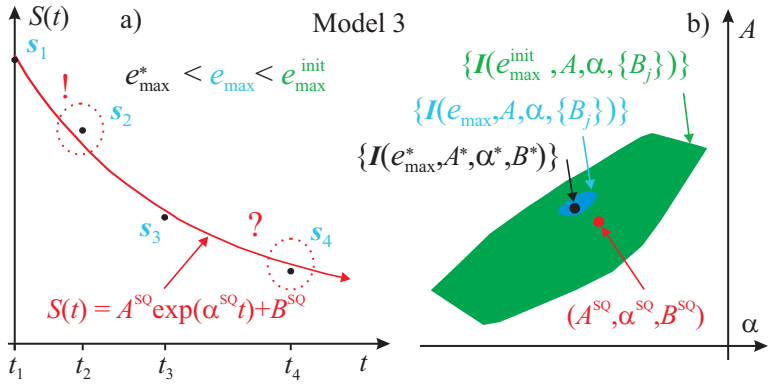

Figure 10: Inadmissible LSQ-solution.

Moreover, this procedure allows one to analyze a common LSQ solution obtained formally, as suggested by Fig. 10. The case is shown for some $e_{\max}$ of the value $e^*_{\max} < e_{\max} < e^{\mathbf{init}}_{\max}$ (elements in blue). The LSQ solution (for Model 3) is inadmissible: the solution (red, Fig. 10a) does not pass *through all* uncertainty intervals $\boldsymbol{s}_n$ (blue), and the point $A^{\mathbf{SQ}}, \alpha^{\mathbf{SQ}}, B^{\mathbf{SQ}}$ (red, Fig. 10b) lies outside the corresponding information set $\boldsymbol{I}(e_{\max}, A, \alpha, B)$ (blue, Fig. 10b). But at the same time, the limit solution (black circle, Fig. 10b) exists for the value $e^*_{\max}$. It is very difficult to compare these two solutions in the process plane (Fig. 10a), but we can do it *constructively* in the space

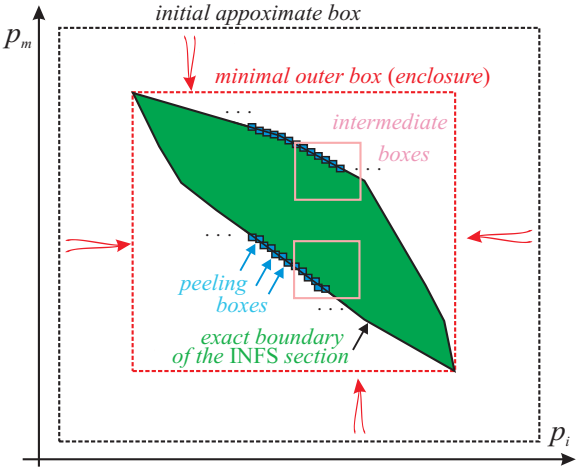

Figure 11: Comparison with the classical parallelotope approach.

of parameters. Notice that a similar technique of bound evaluation is widely applied for solving systems of interval inequalities (see e.g., [10]).

A comparison of these results in Fig. 11 with the classical approach based on enclosure boxes [8]–[10] confirms the idea that applying specific properties of the investigated dependence allows one to construct exact boundaries of the information set and crucially accelerate computations. The approach under discussion is similar to the advanced "strip" method [11], but is faster due to analytical computation of vertices coordinates for the partial information sets (15) and application of fast program of intersection of the convex polygons.

5 Practical Examples

The initial bound on the total corruption (taken quite conservatively) was given by the researcher as $e_{\max}^{\mathbf{init}} = 0.01$ mol/litre. However, for Model 3, estimates of the limiting values $e_{\max}^{*}$ for the actual level of total corruptions are 0.0015, 0.0042, and 0.0050 mol/litre in the experimental samples 1–3 (Fig. 1). Comparison of these values confirms that the experiments have been performed with high accuracy (about 1.0–1.5%).

Next, we consider results of processing the experimental data for the nano-catalyst (Fig. 1, sample 1 in red) using Model 3.

The projection of the INFS sections onto the plane ($\log A$–α) for admissible values of the parameter B is shown in Fig. 12, where $e_{\max} = e_{\max}^{\mathbf{init}} = 0.01$ mol/litre were chosen for computations. Here, the red circle marks the LSQ solution $\log A^{\mathbf{SQ}} = 0.565$, $\alpha^{\mathbf{SQ}} = -0.0718$ 1/min, $B^{\mathbf{SQ}} = 0.085$ mol/litre (as in Fig. 5); and the section in red is one closest to the $B^{\mathbf{SQ}}$-estimate. The INFS spatial image is given in Fig. 13. Its image in the (A–α) plane (in its natural scale) is shown in Fig. 14.

The projection of the INFS image onto the (B–A) plane is given in Fig. 15 (in its natural scale). The projection of the INFS image onto the (B–α) plane is shown in Fig. 16. In these pictures, red circles mark the points of the LSQ solution, while red

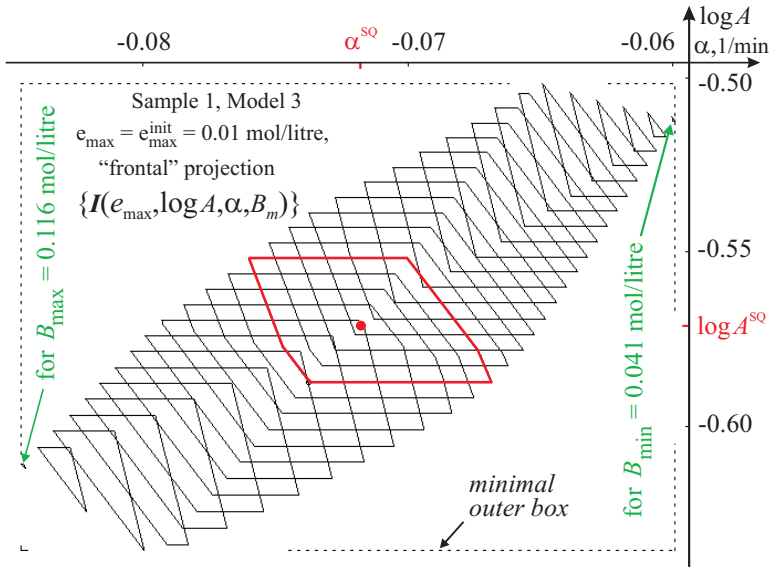

Figure 12: Information set as collection of sections: projection onto the $\log A$–α plane.

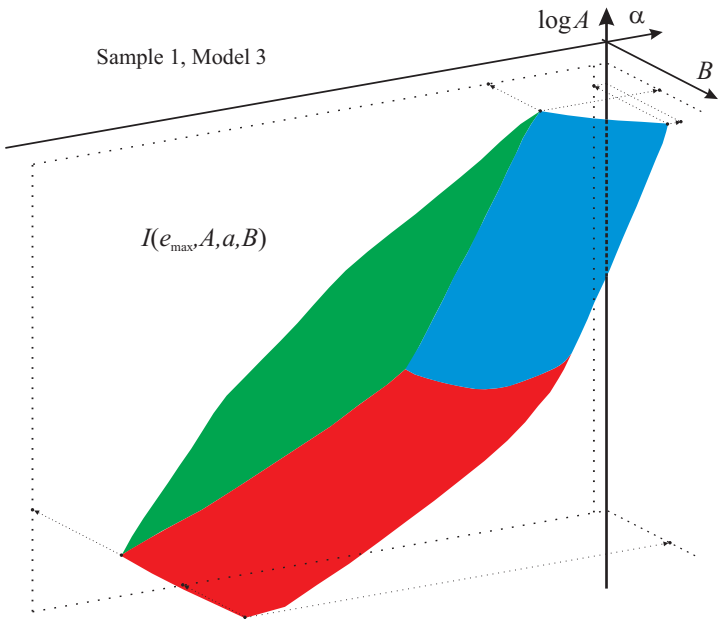

Figure 13: Information set; spacial image.

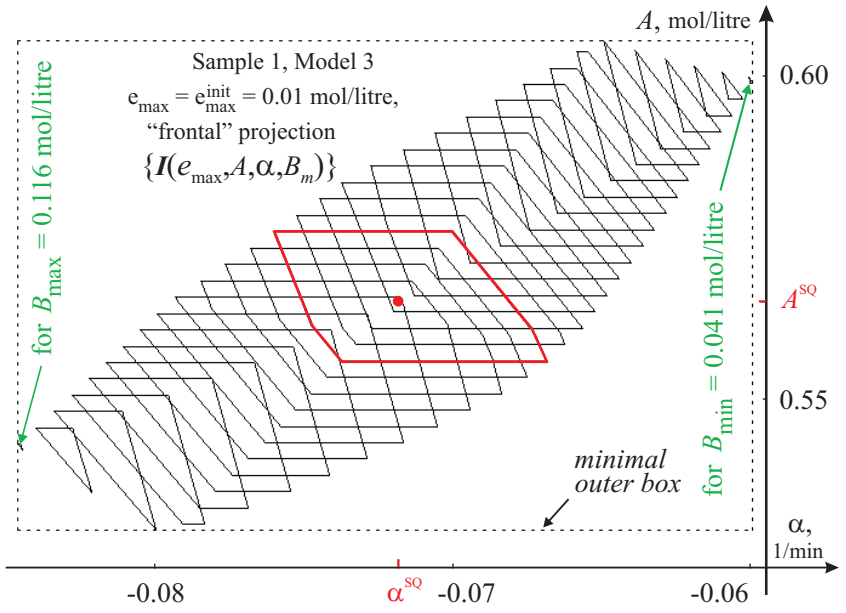

Figure 14: Information set as a collection of sections - projection onto the (A–α) plane, natural scale.

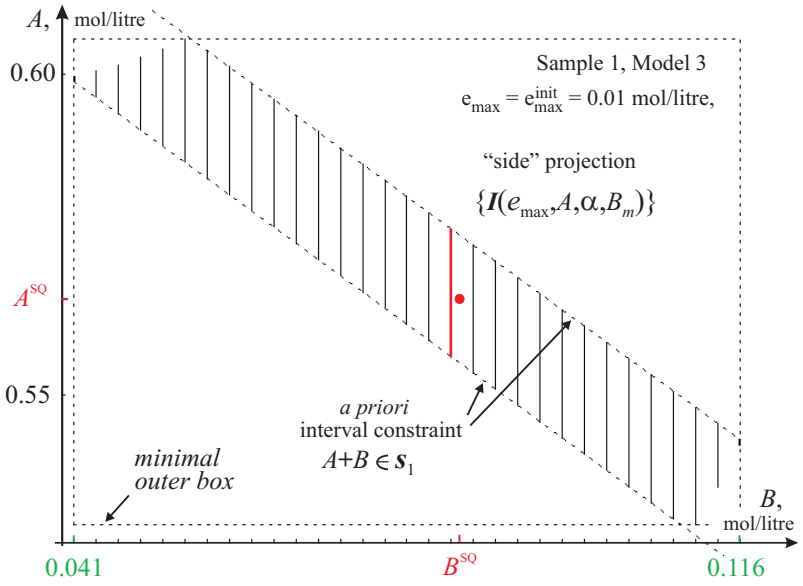

Figure 15: Information set projection onto the (B–A) plane, natural scale.

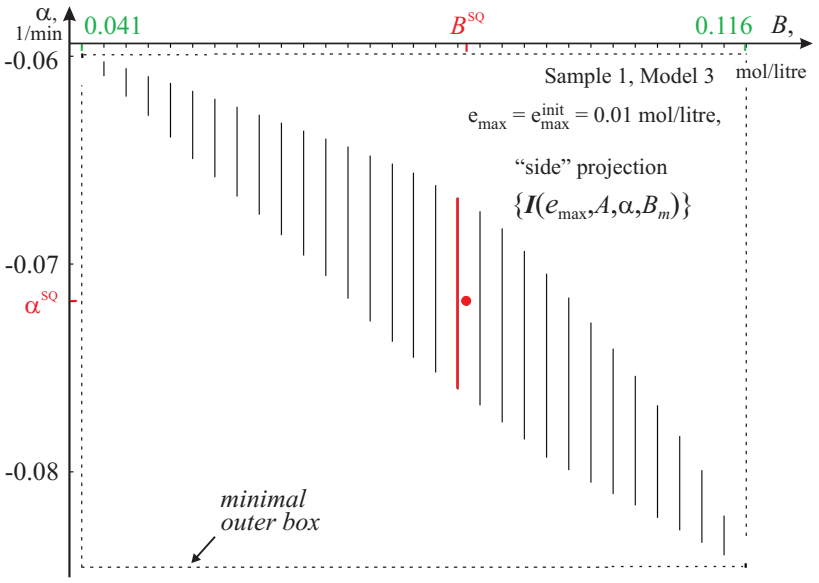

Figure 16: Information set projection onto the the (B–α) plane.

vertical segments are the INFS sections which are nearest to the value of $B^{\mathbf{SQ}}$.

Thus, one may conclude that for the value $e_{\max} = e^{\mathbf{init}}_{\max} = 0.01$ mol/litre chosen for demonstration, the LSQ solution is *admissible*. Moreover, under the uncertainty considered, the LSQ solution is incomplete, since it cannot give such rich information (Figs. 12–16) as we obtain by the interval approach.

Next, we consider results of processing the experimental data for a nano-catalyst (Fig. 1, sample 1 in red) using Model 4. For this model, the algorithms are similar, but for two grids in the parameters B and β. Transforming the initial relation $S(t, A, \alpha, \beta, B) = A\exp(\alpha t + \beta t^2) + B$ into a linear form is performed as follows.

First, we introduce an approximate reasonable interval and grid on the parameter $\{B_m, m = \overline{1, M}\}$ using the results of computations with Model 3:

$$\boldsymbol{B} = [\underline{\boldsymbol{B}}, \overline{\boldsymbol{B}}]: \ \Delta B = (\overline{\boldsymbol{B}} - \underline{\boldsymbol{B}})/(M-1), \ B_m = \underline{\boldsymbol{B}} + \Delta B(m-1), \ m = \overline{1, M}.$$

Second, an approximate reasonable interval and grid on the parameter $\{\beta_k, k = \overline{1, K}\}$ are introduced by taking into account the physical bound $\beta < 0$ on this parameter:

$$\boldsymbol{\beta} = [\underline{\boldsymbol{\beta}}, \overline{\boldsymbol{\beta}}]: \ \Delta\beta = (\overline{\boldsymbol{\beta}} - \underline{\boldsymbol{\beta}})/(M-1), \ \beta_k = \underline{\boldsymbol{\beta}} + \Delta\beta(k-1), \ k = \overline{1, K}.$$

Further, similarly to (13), we obtain for each B_m

$$\log\big(\boldsymbol{s}_n - B_m\big) \ni \log A + \alpha t_n + \beta_k t_n^2, \quad m = \overline{1, M}, \ k = \overline{1, K}, \ n = \overline{1, N}.$$

After transferring the node β_k to the opposite side of the above equality, we obtain for each node B_m and each node β_k the following collection (on t_n) of inclusions for the parameters α and $\log A$:

$$\log A + \alpha t_n \in \log\big(\boldsymbol{s}_n - B_m\big) - \beta_k t_n^2, \quad m = \overline{1, M}, \ k = \overline{1, K}, \ n = \overline{1, N}.$$

Finally, having performed the search over the external grid $\{\beta_k\}$ and the internal grid $\{B_m\}$, we obtain a description of the information set $\boldsymbol{I}(e_{\max}, \log A, \alpha, B_m, \beta_k)$ as a collection of two-dimensional sections over the grids on B and β. The marginal sections of the set $\boldsymbol{I}(e_{\max}, \log A, \alpha, B_m, \beta_k)$ are calculated by appropriate adjustment of the grid $\{B_m\}$, through shifting the position of the interval $\boldsymbol{B} = [\underline{\boldsymbol{B}}, \overline{\boldsymbol{B}}]$, changing the number of nodes M, and by decreasing the step ΔB around these sections. A similar adjustment is performed over the grid $\{\beta_k\}$.

As a result, we obtain information necessary for description and representation of all the INFS sections $\boldsymbol{I}(e_{\max}, \log A, \alpha, B_m, \beta_k)$, $m = \overline{1, M}$ and $k = \overline{1, K}$. The projection of this set onto the plane (β–B) is shown in Fig. 17. Note that each admissible value of β determines a corresponding interval of admissible values of B.

For Model 4, the marginal admissible curve $s(t) = A(\beta_{\min}) \exp\big(\alpha(\beta_{\min})t + \beta_{\min} t^2\big) + \widetilde{B}(\beta_{\min})$ (in red) for the marginal value $A(\beta_{\min}), \alpha(\beta_{\min}), \beta_{\min}, \widetilde{B}(\beta_{\min})$ from the INFS $\boldsymbol{I}(e_{\max}, A, \alpha, \beta, B)$ is shown in Fig. 18 in comparison with the LSQ curve $s^{\mathbf{SQ}}(t) = A^{\mathbf{SQ}} \exp(\alpha^{\mathbf{SQ}} t) + B^{\mathbf{SQ}}$ (in green, by Model 3). A significant difference is seen between these curves, especially in levels of B.

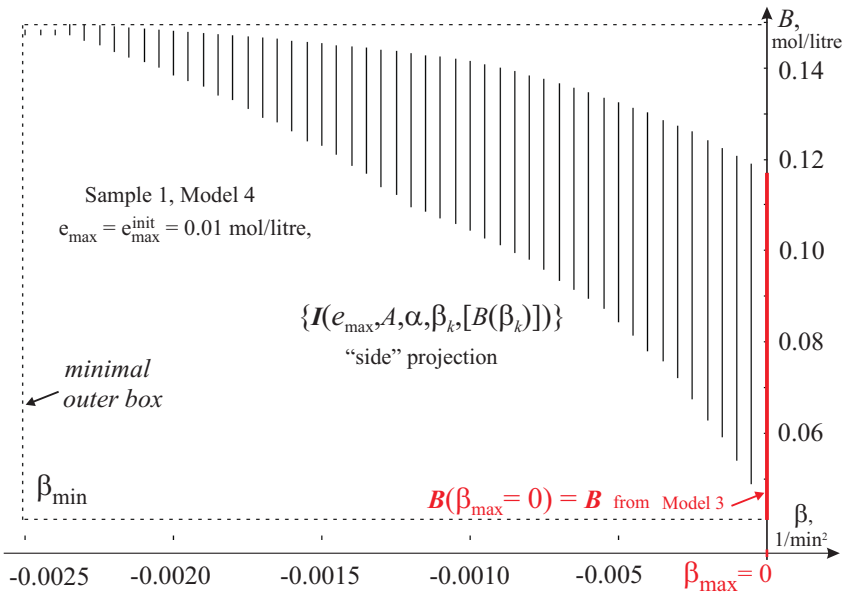

Figure 17: Model 4, sample 1; projection of the information set $I(e_{\max}, \log A, \alpha, B_m, \beta_k)$ onto the plane (β–B).

6 Conclusions

We can conclude that the interval approach overcomes the difficulties of the standard technique and produces a constructive description for the subtle structure of the information set of parameters as well as the minimal guaranteed enclosure for each parameter and a lower estimate for the actual level of the total corruption in the pro-

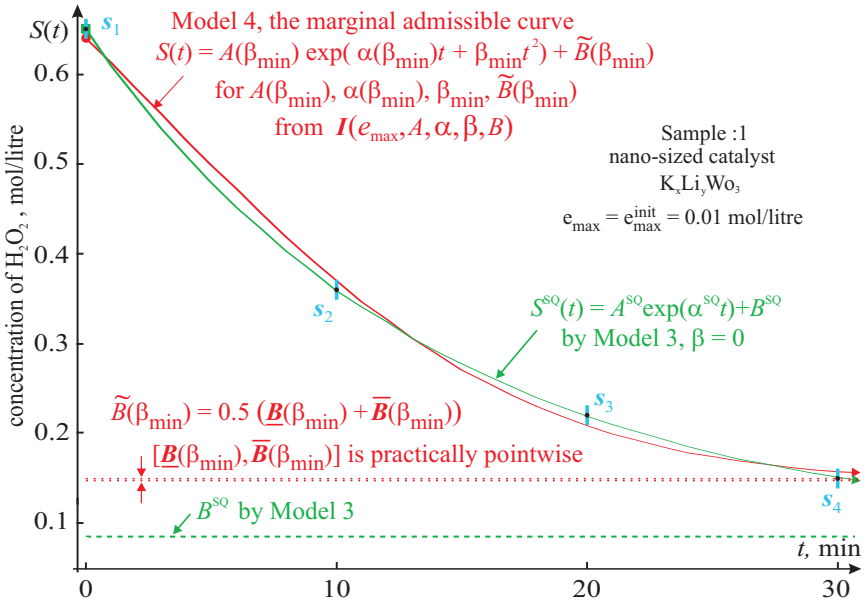

Figure 18: The marginal admissible curve for $A(\beta_{\min}), \alpha(\beta_{\min}), \beta_{\min}, \widetilde{B}(\beta_{\min})$ from the information set $I(e_{\max}, A, \alpha, \beta, B)$.

cessed experimental data. Moreover, this allows one to analyze the validity of various models of the process under study.

In the majority of practical cases, the developed hybrid "grid–analytical" algorithms for constructing the information sets of parameters (together with transformation of variables) result in fast computational procedures that provide exact description of boundaries of information set sections.

For the given experimental data, we use our interval procedure to find the limiting values of the bounds $e^*_{\max}$ on the total measuring error. The bounds were at the level 1.0–1.5%. We conclude that the chaotic components of the measuring error are very small, and the experiments had been performed with very high quality to yield sufficiently accurate results.

Acknowledgments

The authors wish to thank Prof. Sergey P. Shary for attention to the work and for constructive discussion of the results presented in the paper.

References

[1] GOST 8.207-76. *The State System for Providing Uniqueness of Measuring. Direct Measuring with Multiple Observation. Methods for Processing of the Observation Results.* Goststandart, Official Edition, Moscow, Russia, 1976. (in Russian)

[2] MI 2083-93. *Recommendations. The State System for Providing Uniqueness of Measuring. Indirect Measuring. Determination of the Measuring Results and Estimation of their Errors.* Goststandart, Official Edition, Moscow, Russia, 1993. (in Russian)

[3] R 40.2.028–2003. *The State System for Providing Uniqueness of Measuring. Recommendations on Constructing the Calibration Characteristics. Estimation of Errors* (*Uncertainties*) *of Linear Calibration Characteristics by Application of the Least Square Means Method.* Goststandart, Official Edition, Moscow, Russia, 2003. (in Russian)

[4] L.A. Petrov, Yu.V. Mikushina, et. al. Catalytic Activity of Oxide Polycristal and Nano-Sized Tungsten Bronzes Produced by Electrolysis of Molten Salts, *Izvestiya Acad. Nauk, ser. Chemical* 10 (2011), pp. 1951–1954. (in Russian)

[5] I.A. Semiokhin. *Kinetics of Chemical Reactions*, Nauka, Moscow, 1995. (in Russian)

[6] A.P. Purmal'. *Chemical Kinetics*, Nauka, Moscow, 1993. (in Russian)

[7] N.M. Emanuel and D.G. Knorre. *Course of Chemical Kinetics.* Nauka, Moscow, 1984. (in Russian)

[8] E. Hansen and G.W. Walster. *Global Optimization using Interval Analysis.* Marcel Dekker, New-York, Basel, 2004.

[9] L. Jaulin, M. Kieffer, O. Didrit, and E. Walter. *Applied Interval Analysis*, Springer, London, 2001.

[10] S.P. Shary. *Finite-Dimensional Interval Analysis.* Electronic Book. Novosibirsk, XYZ, 2013. Available at:
`http://www.nsc.ru/interval/Library/InteBooks/SharyBook.pdf` (in Russian)

[11] S.I. Zhilin. Simple Method for Outlier Detection in Fitting Experimental Data under Interval Error, *Chemometrics and Intelligent Laboratory Systems*, vol. 88 (2007), No. 1, pp. 60–68.

[12] S.I. Kumkov and Yu.V. Mikushina. Interval Estimation of Activity Parameters of Nano-Sized Catalysts, in *Proc. All-Russian Conference "Statistics, Simulation, and Optimization"*, The Southern-Ural State University, Chelyabinsk, Russia, November 28–December 2, 2011, pp. 141–146. (in Russian)

[13] S.I. Kumkov. Procession of Experimental Data on Ionic Conductivity of Molten Electrolyte by the Interval Analysis Methods, *Rasplavy* 3 (2010), pp. 86–96. (in Russian)

[14] A.M. Potapov, S.I. Kumkov, and Y. Sato. Procession of Experimental Data on Viscosity under One-Sided Character of Measuring Errors, *Rasplavy* 3 (2010), pp. 55–70. (in Russian)

[15] P.A. Arkhipov, S.I. Kumkov, et. al. Estimation of Plumbum Activity in Double-Systems Pb-Sb and Pb-Bi, *Rasplavy* 5 (2012), pp.43–52. (in Russian)

[16] R.B. Kearfott, M.T. Nakao, S.M. Rump, S.P. Shary, and P. van Hentenryck. Standardized Notations in Interval Analysis, *Computational Technologies*, vol. 15 (1) (2010), pp. 7–13; A preliminary version also available at `http://www.nsc.ru/interval/INotation.pdf`